VOLUME - 12, ISSUE - 05, MAY - 2023 • PRINT ISSN No. 2277 - 8160 • DOI : 10.36106/gjra

Original Research Paper

Radiology

FAT-RICH VS FAT-POOR RENAL AML ON MULTIPARAMETRIC MRI.

Dr. Umar Nazir*	MD Department of Radiodiagnosis and Imaging, SKIMS, Srinagar *Corresponding Author
Dr. Mudasir Hamid Bhat	MD Department of Radiodiagnosis and Imaging, SKIMS, Srinagar
Dr. Sehrish Shaheen	MD Department of Radiodiagnosis and Imaging, SKIMS, Srinagar

ABSTRACT

Background: The study aims to show the MRI imaging features of Fat-rich and Fat-poor AML using MULTIPARAMETRIC renal MRI protocol. Fat-poor angiomyolipomas (AMLs) are challenging to differentiate from other renal lesions on USG and CT and often necessitate biopsy or surgery for differentiation. **Methods:** The study group consisted of 9 patients with histologically proven AMLs who underwent MULTIPARAMETRIC renal MRI (T2WI, Chemical Shift imaging, DWI,) before the histopathology. The lesions were reviewed independently by a radiologist and a resident. **Results:** On T2-weighted images, among Fat rich AML (n=2 i.e. 66%) showed heterogeneous hyperintense signal and (n=1 i.e. 33%) showed homogenous hyperintense signal as compared to renal cortex. Among Fat Poor AML (n=4 i.e. 66%) showed homogenous hypointense signal and (n=2 i.e. 33%) showed heterogeneous hypointense signal as compared to renal cortex. On Chemical Shift Imaging, among Fat rich AML, mean Signal Intensity drop (%) on out of phase imaging for Fat rich AML in our study was 27.07%±1.65%. Also Fat rich AML (n=3 i.e. 100%) showed Indian Ink Artifact within the mass or at its interface with the kidney. Among Fat Poor AML, mean Signal Intensity drop (%) on out of phase imaging for Fat poor AML in our study was 0.6%±6.7% (p value <0.001). On Diffusion Weighted Imaging, apparent diffusion coefficient (ADC) maps show low ADC values regardless of the types of AML, because fat signal intensity is suppressed. among Fat rich AML mean ADC values of lesion in our study was 0.86±0.09, Among Fat Poor AML, mean ADC values of lesion in our study was 0.96±0.01. **Conclusion:** Our study enables us to confirm consistent associations of MR imaging features with specific subtypes of AML. In our study, T2 signal intensity, T2 signal intensity ratio, signal drop on out of phase imaging, showed promising results differentiating between fat rich and fat poor AML.

KEYWORDS : Angiomyolipoma, Fat-rich AML, Fat-poor AML, Magnetic resonance Imaging

INTRODUCTION

As there has been increased use of high-resolution cross-sectional imaging, the quantity of incidental renal masses has increased, which requires further imaging for proper diagnosis[1]. In order to distinguish the different renal lesions several imaging parameters have been proposed. The main benign lesion that may be difficult to differentiate from RCC (Renal cell carcinoma) is angiomyolipoma (AMLs), in particular the lipid-poor subtype[2].

Angiomyolipoma

AML is the most common benign solid renal lesion [3,4] These lesions occur most frequently in the 4th–6th decades with prevalence more in women[4] AMLs are composed of variable amounts of dysmorphic blood vessels, smooth muscle components, and mature adipose tissue[3,5]. Most of the AMLs (80% Approximately) are sporadic and incidental; the remaining 20% are associated with tuberous sclerosis complex and lymphangioleiomyomatosis. As there occurs tumor growth, there is an increase in blood flow causing vessel dilatation and pseudoaneurysm formation[6]. On imaging, AMLs are classified as classic AML (fat-rich AML) and fat-poor AML, depending on their appearance. Far-rich AMLs can be diagnosed with relative ease as they have the pathologic hallmark feature of abundant macroscopic fat and are thus identified on cross-sectional imaging [3,4]. However, it may be difficult to differentiate lipid-poor AMLs from RCCs. In cases where other imaging modalities (USG, CT) show nonspecific features, multiparametric MR imaging may be helpful. On MR imaging, classic AMLs show high T1 signal intensity as they have fat content. The macroscopic fat can be seen as a suppression of signal intensity on fat-saturated images and as india ink artifact on opposed-phase images[3,7]. India ink artifact occurs due to the presence of fat and water protons within the same imaging voxel, which results in signal loss and a black line seen at fat-water interfaces[7]. The signal intensity on T2-weighted images depends on the amount of fat content in the lesion. AMLs with high fat content appear relatively hyperintense on T2-weighted images, while lesions with lower fat content appear hypointense[8]. Lipid-poor AMLs account for 5% of AMLs and are typically reported to be small, with an average diameter of 3 cm[3,9]. A lipid-poor AML is pathologically described as an AML containing less than 25% fat cells per high-power field[3,4]. Lipid-poor AMLs are composed mostly of smooth muscle and disordered vascular components[3]. At MR imaging, these lesions are homogeneous and have high signal intensity on T1-weighted images and low signal intensity on T2weighted images due to the presence of abundant smooth muscle. Lipid-poor AMLs may appear as an exophytic[10] nonround lesion without a capsule[11] and may show a drop in signal intensity on opposed-phase images on comparison with inphase images[4,8,9]. AMLs show restricted diffusion with a corresponding low ADC, but restricted diffusion is not specific for AML.

MATERIALS AND METHODS

- The study was conducted at a tertiary care institute in North India over a period of one year.
- This study involved 9 patients.
- Detailed informed consent was taken from the patients before inclusion in the study.
- Study Design: Hospital based descriptive study
- All Magnetic Resonance Imaging (MRI) studies were performed using a 1.5 Tesla MR system (Magnetom Avanto, Siemens Medical Systems, Erlangen, Germany).

The following protocol was used:

Sequence	Plane	Slice thickness (mm)	TR/TE (ms)	Flip angle (degrees)
2D T2w single shot fast spin echo	Axial	4-5 /No Gap	4000/103	111

2D T1w FLASH in/out phase	Axial	4-5/No Gap	100/2.2	70
Diffusion weighted imaging	Axial	4-5/No Gap	5500/70	90
			b-values (b= 50s/mm2 , b=400 s/mm2, and b=800 s/mm2)	

The morphologic traits were evaluated, it includes size, growth pattern (exophytic/endophytic), Images were also reviewed for the characteristics of the lesions on T2-weighted, In-phase, Out of phase and diffusion-weighted images.

(a) Findings On T2W Images -The MRI signal intensities of the lesion were compared with those of the parenchyma of kidney and categorized as hyper-, iso- or hypointense as compared to the renal parenchyma. Tumor homogeneity or heterogeneity was noted. The signal intensity ratios of tumors on T2-weighted images were calculated quantitatively to evaluate the tumor intensities. ROIs were placed on an axial image. Identical regions of interest (ROIs) were placed on the lesion and kidneys, the sizes of ROI were 10–100 mm. ROIs were placed on axial images

Signal intensity ratio = (SI_{tumor}/ SI_{kidney}). Signal Intensity Ratio greater than 1 signify hyperintense lesion whereas less than 1 signify hypointense lesion.

(b) Findings on Chemical shift images: Drop in signal intensity on opposed-phase chemical shift images relative to that of in-phase images was determined for each lesion.

Signal Intensity Drop was calculated using the following formula $SI_{inphase} - SI_{outphase/} SI_{inphase} \times 100$. SI drop >25% was selected as the cut-off representing significant SI drop due to intravoxel lipid content, ensuring this drop was not related to noise or artifacts. Indian ink artifact was also looked for.

(c) Diffusion Changes On DWI: Apparent Diffusion Coefficient (ADC) Values was measured within the lesion as well as within normal appearing renal parenchyma. ADC Ratio was calculated using the following formula

ADC Ratio = $ADC_{Lesion} / ADC_{Normal\ Parenchyma} x\ 100$.

Statistical Analysis:
Data were coded and recorded in MS Excel spreadsheet program. SPSS v25 (IBM Corp.) was used for data analysis. Descriptive statistics were elaborated in the form of means/standard deviations and for continuous variables, and frequencies and percentages for categorical variables. Data were presented in a graphical manner wherever appropriate for data visualization using box-and-whisker plots and column charts for continuous data. Group comparisons for continuously distributed data were made using independent sample 't' test when comparing two groups. If data were found to be non-normally distributed, appropriate non-parametric tests in the form of Wilcoxon Test were used.

A p-value of <0.05 was considered statistically significant.

OBSERVATIONS AND RESULTS

The study was conducted on 9 patients with Small solid renal lesions detected on ultrasonography/computed tomography were evaluated using magnetic resonance imaging with the aim of lesion characterization. The final diagnosis of fat-poor AML was confirmed by histopathology/cytology. Among the remaining cases of Fat-rich AML, final diagnosis was confirmed by characteristic imaging features and ultrasonographic follow-up was done. The mean age of presentation of patients with Angiomyolipoma in our study was 45±9.9 years with a range of 35-65 years and increased prevalence in women (77.7%).

Lesion Type	Fat Rich AML(n=3)	Fat Poor AML(n=6)
Gender		
Male	0 (0.0%)	2 (33.3%)
Female	3 (100.0%)	4 (66.7%)
Location		
Exophytic	2 (66.7%)	4 (66.7%)
Endophytic	1 (33.3%)	2 (33.3%)
Laterality		
Right	1 (33.3%)	3 (50.0%)
Left	2 (66.7%)	3 (50.0%)
Polarity		
Upper Pole	2 (66.7%)	2 (33.3%)
Mid Pole	1 (33.3%)	4 (66.7%)
Lower Pole	0 (0.0%)	0 (0.0%)
MRI T2 Signal homogenity		
Homogenous	1 (33.3%)	4 (66.7%)
Heterogenous	2 (66.7%)	2 (33.3%)
MRI T2 Signal Intensity		
MRI T2 SI Ratio	77.42 ± 14.13	116.35 ± 8.11
<100 (Hypointense)	0 (0.0%)	6 (100.0%)
>100 (Hyperintense)	3 (100.0%)	0 (0.0%)
Chemical Shift Imaging		
InPhase	285.67 ± 37.07	211.67 ± 21.91
Outphase	208.33 ± 27.74	210.00 ± 23.61
Signal intensity Drop (%)	27.07 ± 1.65	0.67 ± 6.68
<25%	0 (0.0%)	6 (100.0%)
>25%	3 (100.0%)	0 (0.0%)
Diffusion Weighted Imaging		
Lesion	0.86 ± 0.09	0.96 ± 0.12
Normal	1.95 ± 0.18	1.98 ± 0.20
ADC Ratio	43.84 ± 1.48	48.84 ± 7.60
<66	3 (100.0%)	6 (100.0%)
>66	0 (0.0%)	0 (0.0%)

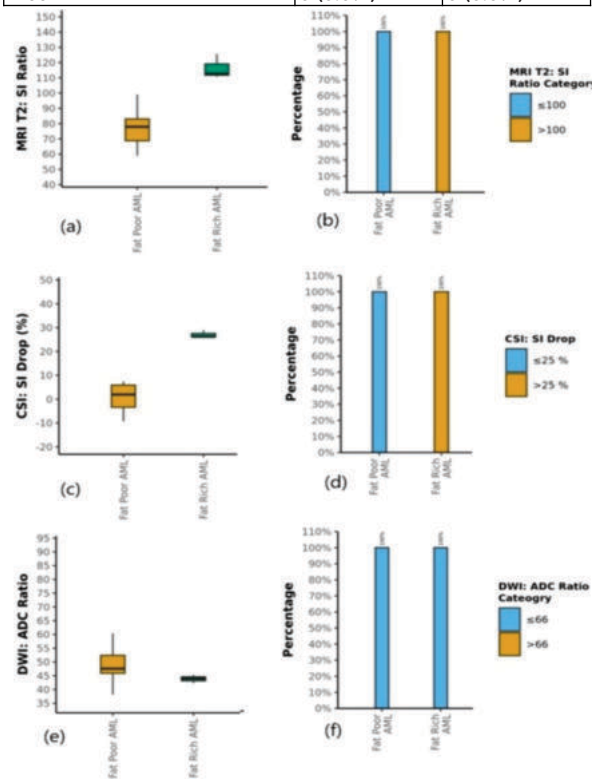

Figure 1. Box plots showing the distribution of (a) MR T2 SI ratio (c) Chemical shift Imaging SI Drop (%) On Out of phase imaging and (e) ADC Ratio. Column graphs showing the comparison of (b) MR T2 SI ratio (d) SI Drop (%) On Out of phase imaging and (f) ADC Ratio between Fat Rich and Fat poor AML.

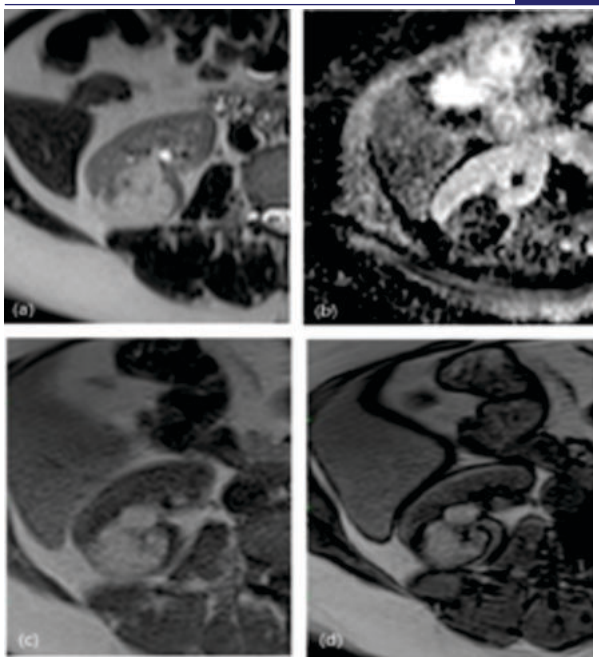

Figure 2: Fat Rich AML in a 45-year-old woman. (a) Axial T2-weighted image shows a 3.9-cm hyperintense renal mass. (b) Axial diffusion-weighted image (b = 800 sec/mm2) shows area of strong restricted diffusion. ADC map shows an ADC of 0.85x10−3 mm2 /sec. (c, d) Axial in-phase (c) and opposed-phase (d) images show india ink artifact on the opposed-phase image with signal drop, consistent with macroscopic fat.

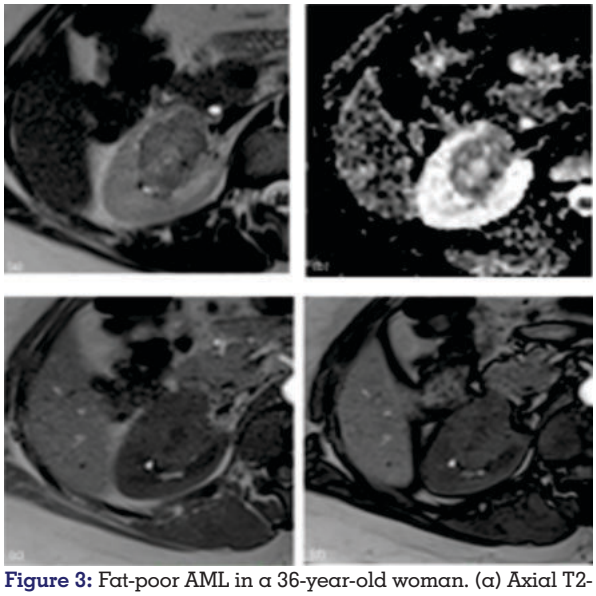

Figure 3: Fat-poor AML in a 36-year-old woman. (a) Axial T2-weighted image shows a 3.9-cm hypointense renal mass. (b) Axial diffusion-weighted image (b = 800 sec/mm2) shows area of strong restricted diffusion. ADC map shows an ADC of 0.95x10−3 mm2 /sec. (c, d) Axial in-phase (c) and opposed-phase (d) T1-weighted images show a mild drop in signal intensity of only 7% on the opposed-phase image.

DISCUSSION

AML is one of the most commonly encountered benign solid renal lesion (Jinzaki M et al[3], Woo S et al[4]). The mean age of presentation of patients with Angiomyolipoma in our study was 45±9.9 years with a range of 35-65 years and increased prevalence in women (77.7%) (Woo S et al[4]).

On T2-weighted images, among Fat rich AML (n=2 i.e. 66%) showed heterogeneous hyperintense signal and (n=1 i.e. 33%) showed homogenous hyperintense signal as compared to renal cortex. None of the cases showed hypo-intense signal on T2-weighted images. Mean Signal Intensity ratio value for Fat rich AML in our study was 116.35±8.11. Among Fat Poor AML (n=4 i.e. 66%) showed homogenous hypointense signal and (n=2 i.e. 33%) showed heterogeneous hypointense signal as compared to renal cortex. None of the cases showed hyperintense signal on T2-weighted images. Mean T2-Signal Intensity ratio value for Fat poor AML in our study was 0.77 ±0.14. Choi HJ et al[12] reported All Fat poor AML were T2-hypointense with T2-SI ratio = 0.61 ±0.10.

On Chemical Shift Imaging, among Fat rich AML mean Signal Intensity on inphase imaging in our study was 285±37 and mean Signal Intensity on out of phase imaging was 208±27 thus Mean Signal Intensity drop (%) on out of phase imaging for Fat rich AML in our study was 27.07%±1.65%. In our study all cases of Fat rich AML (n=3 i.e. 100%) showed Indian Ink Artifact within the mass or at its interface with the kidney. Israel GM et al[7] also reported 100% of fat rich AML showing india ink artifact within the mass or at its interface with the kidney. Among Fat Poor AML, mean Signal Intensity on inphase imaging in our study was 211±21 and mean Signal Intensity on out of phase imaging was 210±23 thus Mean Signal Intensity drop (%) on out of phase imaging for Fat poor AML in our study was 0.6%±6.7% (p value <0.001). Hindman N et al[8] also reported Mean Signal Intensity drop (%) on out of phase imaging for Fat poor AML 8%±4%.

On Diffusion Weighted Imaging, apparent diffusion coefficient (ADC) maps show low ADC values regardless of the types of AML, because fat signal intensity is suppressed. among Fat rich AML mean ADC values of lesion in our study was 0.86±0.09, ADC of normal renal parenchyma 1.95±0.18 and Mean ADC Ratio for Fat rich AML in our study was 0.43±0.01 (p value <0.001). Among Fat Poor AML, mean ADC values of lesion in our study was 0.96±0.01, ADC of normal renal parenchyma 1.98±0.20 and mean ADC ratio for Fat poor AML in our study was 0.48±0.07 (p value <0.001) In common renal lesions, published ADC values of lesion varied from 0.74 to 1.46 in Fat rich AMLs, and 0.67 to 1.26 in fat poor AMLs, respectively

CONCLUSION

MRI is an excellent method in characterizing lesions. In our study, T2 signal intensity, T2 signal intensity ratio, signal drop on out of phase imaging, showed promising results differentiating between fat rich and fat poor AML.

Limitations

The main one is a limited number of study subjects. This can potentially be due to the widespread hesitancy of the surgeon to send the patient with renal AML for MRI and due to the COVID-19 pandemic.

Conflicts Of Interest: Nil

REFERENCES

1. Volpe, A., Panzarella, T., Rendon, R. A., Haider, M. A., Kondylis, F. I., & Jewett, M. A. S. (2004). The natural history of incidentally detected small renal masses. Cancer, 100(4), 738–745. https://doi.org/10.1002/cncr.20025
2. Perez-Ordonez, B., Hamed, G., Campbell, S., Erlandson, R., Russo, P, Gaudin, P, & Reuter, V. (1997). Renal oncocytoma: a clinicopathologic study of 70 cases. The American Journal of Surgical Pathology, 21(8), 871–883. https://doi.org/10.1097/00000478-199708000-00001
3. Jinzaki, M., Silverman, S. G., Akita, H., Nagashima, Y., Mikami, S., & Oya, M. (2014). Renal angiomyolipoma: a radiological classification and update on recent developments in diagnosis and management. Abdominal Imaging, 39(3), 588–604. https://doi.org/10.1007/s00261-014-0083-3
4. Woo, S., & Cho, J. Y. (2015). Imaging findings of common benign renal tumors in the era of small renal masses: differential diagnosis from small renal cell carcinoma: current status and future perspectives. Korean Journal of Radiology: Official Journal of the Korean Radiological Society, 16(1), 99–113. https://doi.org/10.3348/kjr.2015.16.1.99
5. Farrell, C., Noyes, S. L., Tourojman, M., & Lane, B. R. (2015). Renal angiomyolipoma: preoperative identification of atypical fat-poor AML. Current Urology Reports, 16(3), 12. https://doi.org/10.1007/s11934-015-0484-z

6. Yamakado, K., Tanaka, N., Nakagawa, T., Kobayashi, S., Yanagawa, M., & Takeda, K. (2002). Renal angiomyolipoma: relationships between tumor size, aneurysm formation, and rupture. Radiology, 225(1), 78–82. https://doi.org/10.1148/radiol.2251011477
7. Israel, G. M., Hindman, N., Hecht, E., & Krinsky, G. (2005). The use of opposed-phase chemical shift MRI in the diagnosis of renal angiomyolipomas. AJR. American Journal of Roentgenology, 184(6), 1868–1872. https://doi.org/10.2214/ajr.184.6.01841868
8. Hindman, N., Ngo, L., Genega, E. M., Melamed, J., Wei, J., Braza, J. M., Rofsky, N. M., & Pedrosa, I. (2012). Angiomyolipoma with minimal fat: can it be differentiated from clear cell renal cell carcinoma by using standard MR techniques? Radiology, 265(2), 468–477. https://doi.org/10.1148/radiol.12112087
9. Kim, J. K., Park, S.-Y., Shon, J.-H., & Cho, K.-S. (2004). Angiomyolipoma with minimal fat: differentiation from renal cell carcinoma at biphasic helical CT. Radiology, 230(3), 677–684. https://doi.org/10.1148/radiol.2303030003
10. Takahashi, N., Leng, S., Kitajima, K., Gomez-Cardona, D., Thapa, P., Carter, R. E., Leibovich, B. C., Sasiwimonphan, K., Sasaguri, K., & Kawashima, A. (2015). Small (< 4 cm) renal masses: Differentiation of angiomyolipoma without visible fat from renal cell carcinoma using unenhanced and contrast-enhanced CT. AJR. American Journal of Roentgenology, 205(6), 1194–1202. https://doi.org/10.2214/AJR.14.14183
11. Sung, C. K., Kim, S. H., Woo, S., Moon, M. H., Kim, S. Y., Kim, S. H., & Cho, J. Y. (2016). Angiomyolipoma with minimal fat: differentiation of morphological and enhancement features from renal cell carcinoma at CT imaging. Acta Radiologica (Stockholm, Sweden: 1987), 57(9), 1114–1122. https://doi.org/10.1177/0284185115618547
12. Chung, M. S., Choi, H. J., Kim, M.-H., & Cho, K.-S. (2014). Comparison of T2-weighted MRI with and without fat suppression for differentiating renal angiomyolipomas without visible fat from other renal tumors. AJR. American Journal of Roentgenology, 202(4), 765–771. https://doi.org/10.2214/AJR.13.11058